PROCEEDINGS OF SCIENCE

Modelling cosmic rays escaping from RXJ1713.7−3946 - Is it really a PeVatron?

Gavin Rowell,[a,*] **Sabrina Einecke, Robert König, Ryan Burley, Peter Marinos,**[a] **Miroslav Filipovic, Sanja Lazarevic,**[b] **Yasuo Fukui**[c] **and Hidetoshi Sano**[d]

[a] *The University of Adelaide, Adelaide 5005, Australia*
[b] *Western Sydney University, Sydney 2751, Australia*
[c] *Nagoya University, Nagoya 464-8601, Japan*
[d] *Gifu University, Gifu 501-1193, Japan*

E-mail: gavin.rowell@adelaide.edu.au

RXJ 1713.7−3946 is one of the most prominent supernova remnants (SNRs) at high energies, with clearly rim-brightened emission from X-ray to TeV gamma-ray energies. Its relatively young age (1.6 kyr) also makes it a perfect example to search for evidence of escaping cosmic rays up to PeV energies. However, the level of gamma-ray emission that might trace escaping cosmic rays depends heavily on the presence of interstellar medium (ISM) gas clouds around the SNR, the physics of cosmic-ray escape from SNR shocks, and the transport properties of the escaping cosmic rays. We apply here a newly developed 3D model of escaping cosmic rays from RXJ 1713−3946 coupled to the measured molecular and atomic gas at arc-minute scales, to assess the gamma-ray emission at several places around the SNR and its detectability by future gamma-ray facilities such as the Cherenkov Telescope Array (CTA). For some model variants, the predicted emission from one of the ISM clouds (north-west of the SNR) approaches the CTA-South 50 hr sensitivity in the 10 to 20 TeV energy range.

38th International Cosmic Ray Conference (ICRC2023)
26 July - 3 August, 2023
Nagoya, Japan

*Speaker

PoS(ICRC2023)676

1. Introduction

The existence of particle acceleration in the Milky Way has been established for many decades via observations of cosmic rays (CRs) up to the *knee* feature in the PeV energy regime (e.g. [11, 43]). Additionally, the detection of localised and diffuse Galactic gamma-ray emission reaching ∼0.1 PeV in energy and beyond has provided clues as to the nature of multi-PeV particle accelerators (i.e. PeVatrons) in our Galaxy [2, 4–6, 9, 9, 10, 12, 19, 20]. Supernova remnants (SNRs) have for decades believed to be the major sources of Galactic cosmic-rays (e.g. [41]). However their role as PeVatrons is still debated with discussion centering on the ability of SNR shocks to accelerate particles to PeV energies (e.g. [13, 47]). Besides the expectation that supermassive black holes provide PeV particle acceleration (e.g. [1, 6]), additional or alternative PeVatrons are being put forward with several > 50 TeV and PeV gamma-ray sources now linked to pulsar wind nebulae (PWN), pointing to their ability to accelerate PeV electrons [9]. There is also renewed interest in massive stellar clusters as PeVatrons, given their intense winds operating over long time scales > 10^5 yr [8]. The recent reviews by [16, 18] provide an overview of the key questions concerning PeVatrons.

2. Cosmic Rays Escaping SNRs - Looking for PeVatrons

Given the above discussion, there is clear way forward to finally test the notion of SNRs as PeVatrons. In this work, we made use of the idea first put forward by [7] and later by [36, 37] which considers the time- and energy-dependent escape of cosmic rays (CRs) from SNRs as impulsive accelerators. After acceleration from the SNR shock, CRs escape and are assumed to propagate diffusively through the interstellar medium (ISM) [40]. The energy-dependent diffusion coefficient $D \sim E^{\delta}$ for δ in the range 0.3 to 0.7 means that the highest energy CRs propagate the farthest distances from the SNR in a given time. Our focus here is on CR hadrons (hereafter labeled as CRs) for which radiative losses from CR and ISM proton collisions only become noticeable in ISM clouds with high number density $n >> 100\,\mathrm{cm}^{-3}$. After diffusing some distance from the SNR shock, the escaped CRs may collide with ISM protons tens of pc away from the SNR to produce extended gamma-ray emission spatially co-locating with local ISM clouds or clumps. The general ideal of the model has been applied to explain the GeV to TeV emission detected around several mature (> 10^4 yr) SNRs (e.g. [38, 42, 54]). Most recently [52] applied this model in a systematic study of catalogued SNR and ISM cloud combinations to search for PeVatrons via their >100 TeV emission detectable with future TeV facilities like the Cherenkov Telescope Array (CTA) [23].

3. Application to RXJ 1713.7–3946

Our SNR of interest is the young (1600 yr) TeV-bright shell-type SNR RXJ 1713.7−3946 (hereafter, RXJ 1713). RXJ 1713, at ∼1 kpc distance [48, 53], is one of the best-studied SNRs at gamma-ray energies with the latest results from H.E.S.S. resolving the TeV gamma-ray emission down to several arc-minutes and pushing the energy spectrum beyond 30 TeV in energy [3]. H.E.S.S. was also able to show that the TeV emission spatially extended beyond the synchrotron X-ray shell, providing the first evidence for particles beyond the shock front. Whether or not these particles represent those truly escaping from the shock, or those travelling upstream in what is known as

the shock precursor remains to be seen, due to the present sensitivity limits of H.E.S.S. The first application of the escaping CR model to RXJ 1713 was by [21]. They utilised a 3D data cube of ISM gas (over the $V_{\rm lsr}$ range –450 to 450 km/s) from the LAB HI and Nanten CO surveys, with a combined angular resolution of 0.6° and assumed the gas spanned heliocentric distances from 50 pc to 30 kpc. Here, we adapt the escaping CR model to account for CRs escaping the expanding SNR shock (as also done by [54]) and utilise the molecular ^{12}CO(1–0) gas data cube from the more sensitive Nanten2 CO survey [32] with 3′ resolution (FWHM), plus the SGPS HI data [51] at similar resolution. The molecular gas is expected to dominate the ISM in dense clouds although the atomic gas is a significant component at the SNR location [33]. Key aspects of the escaping CR model are shown below with full details given in [27]. The model is also applied to the mature SNR W28 [28] and an earlier 2D variant to the unidentified source HESS J1804−216 [31].

We evaluate the 3D CR density f (cm^{-3}GeV^{-1} units) at radius R' for CRs after they have escaped the SNR ($t > t_{\rm esc}(E)$) via the following:

$$f(E,R',t') \approx \frac{f_0}{\pi^{3/2}R_d^3}\exp\left[-\frac{(\alpha-1)t'}{\tau_{pp}}-\frac{R'^2}{R_d^2}\right]\ (t > t_{\rm esc}(E))\ , \tag{1}$$

where $t' = t - t_{esc}(E)$ for the SNR escape time $t_{\rm esc}(E)$, α is the power law index of the injected CR spectrum, and the diffusion length R_d is given by:

$$R_d(E,t') = 2\sqrt{D(E)t'\frac{\exp(t'\delta/\tau_{pp})-1}{t'\delta/\tau_{pp}}} \tag{2}$$

Here, δ is the diffusion coefficient index as given above and τ_{pp} is the cooling time for CR-ISM collisions. The normalisation f_0 of the CR density accounts for the release of CRs from an expanding SNR shell of radius $R_{\rm SNR}$:

$$f_0 = \frac{\sqrt{\pi}R_d^3}{\left(\sqrt{\pi}R_d^2+2\sqrt{\pi}R_{\rm SNR}^2\right)R_d+4R_{\rm SNR}R_d^2}\ . \tag{3}$$

The escape time is related to Sedov time $t_{\rm Sedov}$ (onset of the Sedov phase of the SNR) via $t_{\rm esc} = t_{\rm Sedov}(p/p_M)^{-1/\beta}$ which is a function of CR momentum p. The SNR radius $R_{\rm SNR}$ is estimated using Eq. 8 of [56]. The maximum CR momentum is set to $p_M = 1$ PeV/c thus assuming the SNR can act as a PeVatron. The Sedov time for an SNR depends on its total energy $E_{\rm SN}$, ejecta mass $M_{\rm ej}$ and density n_0 of the surrounding ISM the SNR expands into. For core-collapse SNRs like RXJ 1713, $t_{\rm Sedov}$ could vary between a few 100 yrs to > 1000 yr (e.g. see Eq. 7 of [59]). Thus for a young SNR like RXJ 1713, $t_{\rm Sedov}$ will have a significant effect on the level of escaping CRs, and in fact the SNR could still be in the initial free-expansion phase (e.g. [60]).

Assuming $n_0 = 0.5\,{\rm cm}^{-3}$, $E_{\rm SN} = 3\times10^{51}$ erg and $M_{\rm ej} = 5{\rm M}_\odot$ we arrive at $t_{\rm Sedov} \sim 650$ yr and $R_{\rm SNR} = 8.6$ pc (to match the observed SNR X-ray outer shock at 1 kpc). Similarly, the β parameter (often assumed to be 2.5) varying with the magnetic field turbulence evolution will also play an important role [22]. Following [35] we characterise the diffusion coefficient as:

$$D(E) = \chi D_0\left(\frac{E/{\rm GeV}}{B/3\mu{\rm G}}\right)^{\delta} \tag{4}$$

where the suppression factor χ characterises the ISM turbulence, D_0 is the reference diffusion coefficient $D_0 = 3 \times 10^{27}$ cm^2/s at $E = 1$ GeV, $\delta = 0.5$ [14], and B is the magnetic field.

The model also accounts for those CRs that have not escaped by considering them as trapped inside the SNR. A certain fraction $f_{\rm shell} = 0.68$ of these trapped CRs can then be distributed inside the shock as a shell of width $W_{\rm shell}$=3.7 pc according to more detailed diffusive shock acceleration studies of CR confinement (e.g. [15]). In this way, the sum of the trapped and escaped CR energy budgets (converted to gamma-ray emission via the methods outlined in [45, 46]) is given by $E_{\rm SN}$ at all times, and the gamma-ray emission from trapped CRs can be used as a crosscheck against the observed spectra overlapping the SNR, thus helping to constrain the parameter space of the model.

Fig. 1 shows the Nanten2 ^{12}CO(1–0) cube integrated in the kinematic velocity range –15 to 0 km/s, encompassing the 1 kpc distance of RXJ 1713, as well as a tiled 3D view of the cube. Four molecular features (labeled NW, SW, SE, NE) are identified around RXJ 1713 that all have broad ($\Delta V > 20$ km/s) CO spectra. The NW, NE and SE features have peak CO emission $V_{\rm peak} \sim -10$ to –5 km/s, perfectly overlapping the kinematic systemic velocity of RXJ 1713 (~ -7.5 km/s). The SW feature peaks in the slightly different $V_{\rm lsr}$ range -15 to -10 km/s and thus might lie behind RXJ 1713. We note the supershell SG 347.3–0.5–21 situated at 2.5 to 3 kpc distance [49, 53] creates a prominent CO void that becomes quite apparent when looking at wider velocity ranges, e.g. –30 to 0 km/s. The NW position is in fact the star formation region RCW 120 formally placed at 1.3 kpc distance (although the broadness of the CO spectra could infer a 10% to 20% uncertainty on this) and may originate from a cloud-cloud collision scenario [58]. Given the broadness of all four features reflecting local gas motions, and the fact they lie towards the near side of the Sagittarius arm (RXJ 1713 is in fact placed at the front edge of this arm [53]) suggests they could be within a few 100 pc distance of RXJ 1713 and thus potential targets for escaping CRs.

In applying the escaping CR model to RXJ 1713, we set up the ISM gas as the sum of the molecular (CO) and atomic (HI) column densities initially with a 3D region of physical depth $L = 52$ pc discretised along the line of sight (z-axis) to create an array of voxels (3D pixels) as the target ISM. A depth $L = 52$ pc matches the length of the cube along the Galactic latitude and longitude axes so that the various cloud features have similar physical depths to their widths and lengths. Overall, the above set of parameters, adopted by previous studies such as those mentioned earlier, defines our so-called baseline model (see Fig. 2).

4. Baseline Model Results

Fig. 2 shows results when applying the baseline model to RXJ 1713. We can see that the "Model-SNR" prediction from predominantly trapped CRs within a radius 0.6° centred on the SNR (this regions intercepts some gamma-ray emission from escaping CRs fore- and background to the SNR) is within 50% of the SNR TeV emission observed by H.E.S.S. [3]. This is sufficient to account for a 50% leptonic fraction (via inverse-Compton emission) as suggested by [34]. We note though, varying levels of leptonic and hadronic components for the SNR emission have been suggested across the GeV to TeV bands (e.g. [3, 26, 29, 39, 57, 61]), including most recently, a significant contribution from re-accelerated electrons drawn from the Galactic thermal pool [17] (when assuming an ambient density of $n \sim 10^{-2}$ cm^{-3}). This re-accelerated component will depend heavily on the level of Galactic electrons locally inside the pre-supernova wind bubble.

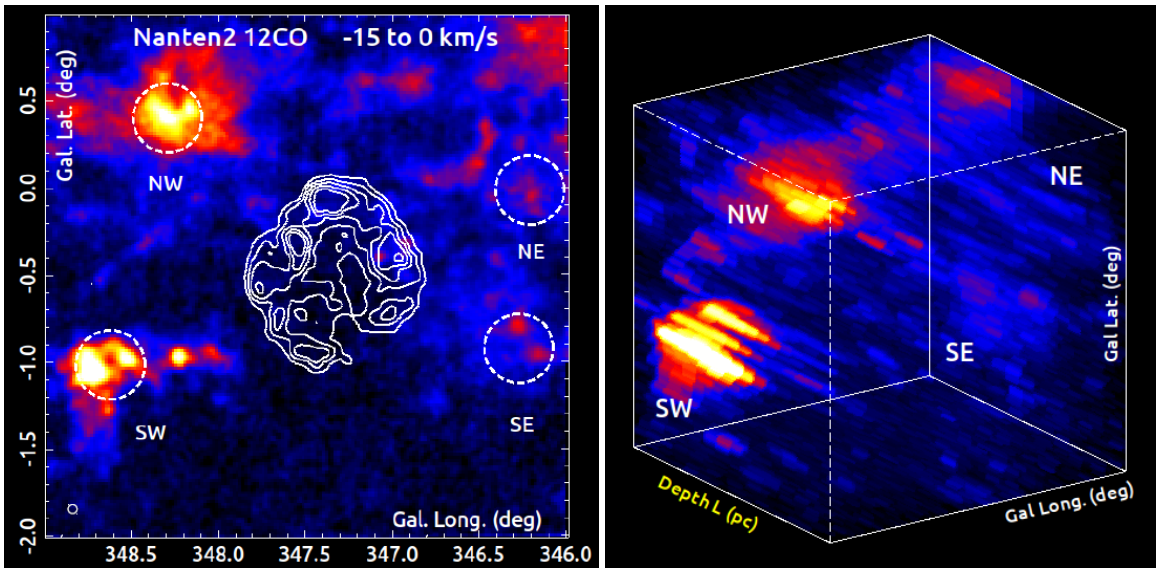

Figure 1: LEFT: Nanten2 ^{12}CO(1–0) image (K km/s units, max level at 99%) integrated over the –15 to 0 km/s range of kinematic velocity $V_{\rm lsr}$. H.E.S.S. > 2 TeV significance contours (10, 15, 20, 25, 30σ) from RXJ 1713.7−3946 [3] are shown as white lines. White dashed circles indicate regions (radius 0.2°) selected for examination by our escaping CR model (see text). The Nanten2 ^{12}CO(1–0) resolution (3′ FWHM) is the solid white circle at the bottom left. **RIGHT**: Tilted 3D view of the Nanten2 ^{12}CO(1–0) cube spanning the –15 to 0 km/s velocity range (z-axis into page, defining the depth L (pc) used in our model). Note that the bottom right side is towards Earth (near side). The SW gas feature appears towards the far side of the cube compared to the other features (NW, NE, SE) which peak closer to the z-axis centre.

Overall though, our Model-SNR spectrum closely matches the observed spectral shape > 0.2 TeV from the SNR without requiring a forced cutoff in the parent particle spectrum. The gamma-ray spectral cutoff >10 TeV from the SNR is quite naturally explained by the escape of higher-energy CRs (the same effect for SNRs in general was also highlighted by [36]). We are at present not considering the hard-spectrum < 0.1 TeV emission measured by *Fermi*-LAT [30] as this may be heavily influenced by the energy-dependent interaction of CRs with the highly clumped ISM measured in and immediately around the SNR (e.g. [39, 44, 50, 55]). This effect could be included in our model as an energy-dependent ambient density that CRs effectively interact with, but this is left as future work.

The model predictions from escaping CRs at the four ISM clouds labeled 'Model-NW' for the NW region and so on, all peak in the 10–100 TeV range as expected due to the energy-dependent diffusion experienced by CRs as they travel the 10–15 pc to these clouds. However, the predicted gamma-ray spectra all fall below the CTA-South 50 hr sensitivity adjusted for the 0.2° region radii. The NW and SW region predictions are the highest due to their large ISM masses > 10^4 M$_\odot$.

5. Some Variations to the Baseline Model

To initially explore the model sensitivity, we looked at some variations in the parameters χ, $M_{\rm ej}$ and L which all have considerable uncertainty and can have major influences on the level of escaping CRs. For a 1 kpc distance the SNR shock radius is required to be $R_{\rm SNR} \sim 8.6$ pc to

1600 yr	Age of SNR accelerator
$n_0 = 0.5/\mathrm{cm}^3$	ISM density of cavity the SNR expands into.
$D_o = 3 \times 10^{27}$ cm^2/s	Diffusion coefficent at 1 GeV.
$\chi = 0.1$	Diffusion suppression factor.
$B = 3$ μG	Magnetic field.
$\delta = 0.5$	Diffusion index.
$\beta = 2.5$	Escape time index.
$E_{SN} = 3 \times 10^{51}$erg	SNR kinetic energy.
$\eta = 0.05$	CR efficiency - Fraction of SNR kinetic energy into CRs.
$M_{ej} = 5 M_{Sun}$	SNR ejecta mass.
$\alpha = 2.1$	CR injection power law index with maximum energy 1 PeV
$W_{shell} = 3.7$ pc	Width of SNR shell for 'trapped' CRs inside (Brose etal 2021).
$f_{shell} = 0.68$	Fraction of trapped CRs inside shell.
L = 52 pc	ISM cube depth along z-axis

$t_{Sedov} \sim 650$ yr
$R_{SNR} \sim 8.6$ pc

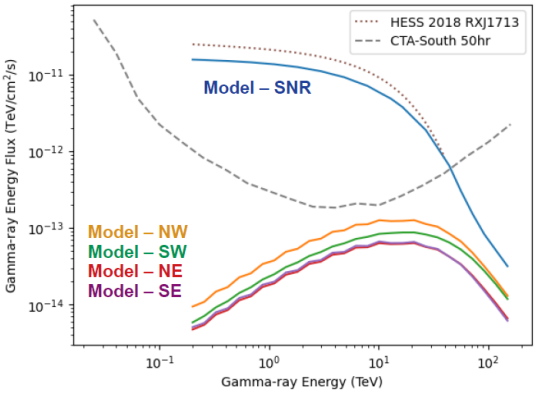

Figure 2: LEFT: Baseline parameters for our escaping CR model, with indicated t_{Sedov} and SNR shock radius R_{SNR}. **RIGHT**: Baseline escaping CR model results for the NW, SW, NE, SE regions (radius 0.2°, labeled "Model-NW" etc. respectively). To compare directly with H.E.S.S. [3] and crosscheck our model, we also include the model results for the SNR (radius 0.6°, "Model-SNR") from the trapped CRs that have not yet escaped. Also included is the CTA-South 50 hr sensitivity from [23] scaled to a region of radius 0.2°.

match the observed radio/X-ray/gamma-ray boundaries. This then imposes some constraints on the combination of n_0, M_{ej} and E_{SN} via the derivation of R_{SNR} as per Eq. 8 of [56] and also the Sedov time t_{Sedov} via Eq. 7 of [59]. An additional constraint comes from the model's predicted "Model-SNR" emission from the trapped CRs inside the SNR, which should roughly match the observed flux as seen by H.E.S.S. [3] to within a factor of ~50% as explained earlier.

Three model variations were tested with results shown in Fig. 3 – (1) $\chi = 0.02$, which alternatively can be achieved with $B = 75\mu$G; (2) $M_{\mathrm{ej}} = M_{\odot}$ which predicts $t_{\mathrm{Sedov}} = 1160$ yr; (3) $L = 100$ pc and $\eta = 0.1$. Model 1 represents slow diffusion into a turbulent ISM which limits the propagation of the escaping CRs, and shows a slight excess of >20 TeV Model-SNR emission (above the observed emission) due to higher-energy escaped particles being locally confined in front of and behind the SNR. Model 2 predicts a Sedov time roughly 2x higher compared to the baseline model and shows a very strong excess in >10 TeV Model-SNR emission since higher-energy particles have not yet escaped. Model 3 expands the ISM cube 2x larger in depth (resulting in 2x lower ISM densities) and thus requires 2x higher CR efficiency $\eta = 0.1$ from the SNR to maintain the Model-SNR emission close to the baseline result. Models 1 and 3 provide the largest escaping CR predictions and in these cases the NW cloud emission is close the CTA-South 50 hr sensitivity.

6. Conclusions

We have applied an escaping CR model in 3D to the young TeV-bright SNR RXJ 1713.7−3946 to investigate the potential gamma-ray emission from local ISM clouds assumed to be within ~20 pc of the SNR. Our model predicts hadronic gamma-ray emission from CRs escaping the SNR and from those still trapped inside the SNR after they interact with the observed ISM gas. The baseline model assumes the SNR accelerates CRs in a pure-power law distribution up to 1 PeV, and other parameters were chosen to ensure the gamma-ray emission from trapped CRs was within ~50%

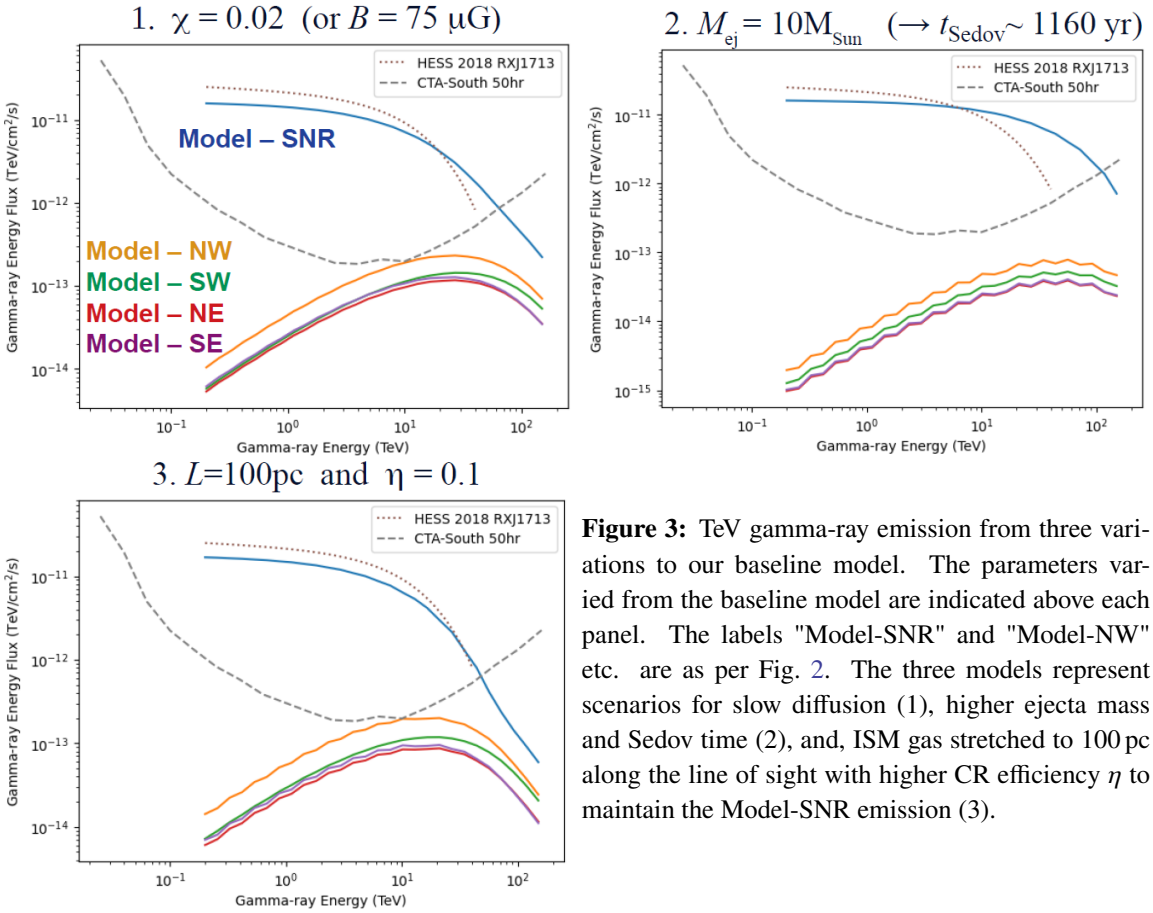

Figure 3: TeV gamma-ray emission from three variations to our baseline model. The parameters varied from the baseline model are indicated above each panel. The labels "Model-SNR" and "Model-NW" etc. are as per Fig. 2. The three models represent scenarios for slow diffusion (1), higher ejecta mass and Sedov time (2), and, ISM gas stretched to 100 pc along the line of sight with higher CR efficiency η to maintain the Model-SNR emission (3).

of the observed TeV emission. Interestingly, the model is able to replicate the observed cutoff at 10-20 TeV energies in the observed SNR spectrum which is dominated by trapped CRs.

Variations to the baseline model were tested, changing (1) diffusion suppression, (2) ejecta mass, and (3) the physical length of the ISM gas along the line of sight and CR acceleration efficiency. In some cases (variations 1 and 3) the gamma-ray emission from a large cloud northwest of RXJ 1713 (the RCW 120 star formation region) just reached the CTA-South 50 hr sensitivity at ∼10 TeV, highlighting the potential for CTA to test the PeVatron nature of RXJ 1713.

Further variations of the parameter space will be tested and the predicted gamma-ray morphology at the ISM clouds will be examined against the CTA-South performance. The present model is limited to a constant diffusion coefficent via constant B and χ values in Eqn.4. However these parameters are expected to vary considerably with the ISM gas parameters (e.g. [24]). Different zones of diffusion will therefore be considered in future model variants. Finally, a key uncertainty concerns the 3D arrangement of the ISM gas clouds. Our model currently stretches the ISM clouds along a fixed depth which can artificially distort their 3D shape in the z-axis. Future work will look at better ways to identify ISM clouds (e.g. via hierarchial dendrograms) as contiguous 3D structures allowing more flexibility in their placement.

References

[1] Abbasi R. et al. 2022 Nature 378, 538
[2] Abbasi R. et al. 2023 Science 380, 6652
[3] Abdalla H. et al. 2018 A & A 612, A6
[4] Abdalla H. et al. 2021 A & A 653, A152
[5] Abeysekara A. et al. 2020 PRL 124 021102
[6] Abramowski A., et al. 2016 Nature 531, 476
[7] Aharonian F. et al. 1996 A & A 309, 917
[8] Aharonian F. et al. 2019 Nat. Astron. 3, 561
[9] Albert A. et al. 2021 ApJL 811, L27
[10] Albert A. et al. 2021 ApJL 907, L30
[11] Amato E., Casanova S. 2021 J. Plasma Phys. 87, 845870101
[12] Amenomori M. et al. 2021 PRL 126, 141101
[13] Bell A. 2004 MNRAS 353, 550
[14] Berezinsky V., et al.: *Astrophysics of Cosmic Rays* North-Holland, Amsterdam (1990)
[15] Brose R. et al. 2021 A&A 654, 139
[16] Casanova S. et al. 2022 Universe 8, 505
[17] Cristofari P. et al. 2021 MNRAS 508, 2204
[18] Cristofari P. 2022 Universe 7, 324
[19] Cao Z. et al. 2021 Nature 594, 7861
[20] Cao Z. et al. 2023 arXiv:2305.05372
[21] Casanova S. et al. 2010 PASJ 62, 1127
[22] Celli S. et al. 2019 MNRAS 490, 4317
[23] `https://www.cta-observatory.org/`
[24] Crutcher R. et al. 2010 ApJ 725, 466
[25] de Oña Wilhelmi E. et al. 2022 ApJL 930, L2
[26] Dermer C., Powale G., 2013, A&A 553, A34
[27] Einecke S. et al. 2023 POS (ICRC 2023) 925
[28] Einecke S. et al. 2023 POS (ICRC 2023) 923
[29] Ellison D. C. et al. 2012 ApJ 744, 39
[30] Federici S. et al. 2015 A&A 577, A12
[31] Feijen K. et al. 2022 MNRAS 511, 5915
[32] Fukui Y. et al. 2006 in 26th IAU Meeting, Special Session 1, SPS1, id.21
[33] Fukui Y. et al. 2012 ApJ 746, 82
[34] Fukui Y. et al. 2021 ApJ 915, 84
[35] Gabici S. et al. 2007 Astrophys Space Sci 309, 365
[36] Gabici S., Aharonian F. 2007 ApJ 665, L131
[37] Gabici S. et al. 2009 MNRAS 396, 1629
[38] Gabici S., et al. 2010 Proc. French Soc. Astron. 313
[39] Gabici S., Aharonian F. 2014 MNRAS 445, L70
[40] Gabici S., Aharonian F. 2007 ApJ 665, L131
[41] Ginzburg V.L., Syrovatskii S.I. 1964 *Origin of Cosmic Rays* Pergammon Press, London
[42] Hanabata Y. et al 2014 ApJ 786, 145
[43] Hillas M. 1984 ARAA 22, 425
[44] Inoue T. et al. 2012 ApJ 744, 71
[45] Kelner S. et al. 2006 Phys. Rev. D 74, 034018
[46] Kafexhiu E. et al. 2014 Phys. Rev. D 90, 123014
[47] Lagage P., Cesarksy C. 1983 A & A 125, 249
[48] Leike R. et al. 2021 Nat. Astron. 5, 832
[49] Matsunaga K. et al. 2001 PASJ 53, 1003
[50] Maxted N. et al. 2013 PASA 30, e055
[51] McClure-Griffiths N. et al. 2005 ApJSupp 158, 178
[52] Mitchell A. et al. 2021 MNRAS 503, 3522
[53] Moriguchi Y. et al. 2005 ApJ 631, 947
[54] Ohira Y. et al. 2011 MNRAS 410, 1577
[55] Sano H. et al. 2020 ApJ 904, L24
[56] Reynolds J. 2008 ARAA 46, 89
[57] Tanaka T. et al. 2008 ApJ 685, 988
[58] Torii K. et al. 2015 ApJ 806, 7
[59] Truelove J., McKee C. 1999. ApJSupp 120, 299
[60] Tsuji N. et al. 2019 ApJ 877, 96
[61] Zirakashivili V., Aharonian F. 2010 ApJ 708, 965